Studies on preparation, characterization and antibacterial properties of CuO substituted 45S5 bioglass as bioactive ceramic material

6.1 Introduction

Various types of bioactive materials have been developed over the last three decades. Amongst these, the main bioactive materials used clinically are bioactive glasses in the SiO_2 - Na_2O - CaO - P_2O_5 system (Ogino and Hench, 1980), bioactive glass–ceramic, A - W containing crystalline oxyfluoroapatite [$Ca_{10}(PO_4)_6(O, F)_2$] and β - wollastonite [$CaO.SiO_2$] in a MgO - CaO - SiO_2 glassy matrix (Kokubo *et al*., 1990), hydroxyapatite (HA) [$Ca_{10}(PO_4)_6(OH)_2$] (Jarcho *et al*., 1977) and β - tricalcium phosphate (TCP) [$Ca_3(PO_4)_2$] (Rejda *et al*., 1977). A bioactive material is considered as the one that elicits a specific biological response at the interface that results in the formation of a bond between tissues and the materials (Hench and Anderson, 1993). The most widely researched bioactive material is 45S5 bioactive glass [composition: wt. %: 45 SiO_2 - 24.5 Na_2O - 24.5 CaO - 6 P_2O_5], where S denotes the network former SiO_2 in 45% by weight followed by a specific Ca/P molar ratio 5.2 (Best *et al*., 2008). It was invented by Hench in 1969. The 45S5 bioactive glass is biocompatible and shows high bioactivity which is in fact clinically used for middle ear prostheses and as endosseous ridge implants (Aina *et al*., 2009). Its bioactivity is characterized by the apatite forming ability on the surface upon immersion in physiological fluid (Ohtsuki *et al*., 1992). This has rendered BG its wide use in bone regeneration field, for example periodontal disease (Srinivasan *et al*., 2012), coatings of implants (Mazrooei and Fathi, 2011) and scaffolds (Chen *et al*., 2006).

Clinically, bacterial colonization or infections pose a serious threat to the use of implants and often leads to their failure (Pye *et al*., 2009). Although some BG have been reported to possess antibacterial properties, it is more advantageous to modify BG by incorporating some useful elements into its structure in order to control the release of these ions which are responsible for the antibacterial activity (Hoppe *et al*., 2011).

Metals such as silver (Ag), gold (Au), copper (Cu) and zinc (Zn) are well known for their antibacterial activities (Schrand *et al*., 2010) and are used for a number of *in vitro* and *in vivo* applications. Silver has been used to prevent bacterial colonization of prostheses (Gosheger *et al*., 2004), catheters (Rupp *et al*., 2004) and human skin (Lee and Jeong, 2005). In hospitals, copper alloys, used in doorknobs and other surfaces, exerted an *in vitro* antimicrobial effect against Escherichia coli O157, methicillin-resistant *Staphylococcus aureus* (MRSA) and *Clostridium difficile* while equivalent stainless steel surfaces did not (Grass *et al*., 2011, Espirito Santo *et al*., 2008 and Noyce *et al*., 2006). Copper and zinc amalgams have proven useful in dental materials (Santo *et al*., 2008) where as their salts have been incorporated into mouthwashes for the treatment of gingivitis (Morrier *et al*., 1998).

Copper is essential for human life forming part in enzymes of great importance for the normal functioning of the body (Arredondo *et al*., 2005). It is an angiogenic agent because of that increases the expression of pro-angiogenic and growth factors (VEGFs), enhances the *in vivo* angiogenesis, and stimulates the human endothelial cell proliferation (Lakhkar *et al*., 2012, Finney *et al*., 2009 and Gérard *et al*., 2010). Cu has been incorporated in various materials used in biomedical applications showing anti-bacterial and angiogenic properties, and a role in collagen deposition, cellular activity and

proliferation of osteoblasts (Varmette *et al*., 2009, Srivastava *et al*., 2012 and Palza *et al*., 2013). The *in vitro* bioactivity of Cu-doped glasses was dependent on the concentration of metal ion incorporated which inhibited the formation of apatite at higher concentrations (Erol *et al*., 2013). The incorporation of Cu also increased the chemical durability and mechanical strength of the glasses (Srivastava *et al*., 2012) and promoted an anti-inflammatory prophylactic effect (Varmette *et al*., 2009).

Despite the above mentioned properties, more studies relating to the microstructure and the composition of Cu doped bioactive glasses with their apatite forming ability, their antibacterial effect and biological performance are necessary. The aim of present investigation is to determine the bioactive behavior of 45S5 bioactive glass by exploiting its compositional flexibility with CuO. Therefore, in the present investigation, the 45S5 bioactive glass has been taken as a reference glass. The concentration of CaO was varied by mol% addition of CuO from 0.5-2.5 mol%, respectively in the 45S5 bioactive glass. The purpose of this work is to provide information on bioactivity assessment and to increase the other physical as well as mechanical properties and to create antibacterial effect in 45S5 bioglass by introducing 0.5-2.5 mol% CuO into it.

6.2 Materials and methods

6.2.1 Sample preparation

The mol% compositions of the bioglass samples are shown in Table 6.1. Fine-grained quartz was used for silica (SiO_2). Analytical reagent grade calcium carbonate ($CaCO_3$),

sodium carbonate (Na_2CO_3) and ammonium dihydrogen orthophosphate ($NH_4H_2PO_4$) (Merck specialities private limited, Mumbai, India, Assay 99.8%) were used as a source of CaO, Na_2O and P_2O_5, respectively. The required amounts of analytical reagent grade (Merck specialities private limited, Mumbai, India, Assay 99.8%) CuO was added in the batch for the partial substitution of CaO. The proper raw materials for different samples were weighed. The mixing of different batches was done for 30 minutes and then melted in 100 ml platinum-2% rhodium crucibles. The thermal cycle was set for all the glass samples from room temperature to 1000°C at the rate of 10°C/min. Further, it was held at 1000°C for one hour and heated from 1000°C to 1400°C at the rate of 10°C/min and again held at 1400°C for two hours. The melting of the samples was done in the electric globar furnace in air as furnace atmosphere. The glass melt was taken out of the furnace, poured in a pre-heated rectangular stainless steel mould kept on the steel plate. The glass samples were properly annealed at 500°C for 1h and cooled slowly to room temperature with a controlled rate of cooling inside the muffle furnace to remove the thermal stress and strain from the glass. A part of the annealed bioactive glass samples was cut, ground and polished for measurement of its physical and mechanical properties. The other parts of the glass samples were crushed in a pestle mortar and then ground in an agate mortar to make fine powders for measurements of its bioactivity, structural determination and other properties using various experimental techniques such as XRD, FTIR spectrometry, SEM analysis and pH measurements. To evaluate the bioactivity of the glass samples, *in vitro* tests were performed according to the method described by Kokubo and Takadama (Kokubo *et al*., 2006) using SBF solution with a sample mass to volume of SBF ratio as 0.01 g ml^{-1}.

6.2.2 Antibacterial tests

Antibacterial properties of the samples (45S5, Cu-1, Cu-2 and Cu-3) were investigated using quantitative viable count method. The stock solution was prepared by mixing 1 mL E. coli with 9 mL of LB (Luria- Bertani) broth and incubated at 37°C for 24 h with shaking at 250 rpm. 0.1 g BG powder was autoclaved and mixed with the stock solution. 0.1 mL of the prepared mixture was then inoculated on LB agar plates followed by incubation at 37°C for 24 h. Finally, the number of colony-forming units was counted. The tests were carried out in triplicate. Student's t-test was used to evaluate the statistical significance amongst the data.

Table 6.1: Mol% composition of bioactive glass samples.

Sl. No.	SAMPLE	SiO_2	Na_2O	CaO	P_2O_5	CuO
1.	45S5	46.1	24.4	26.9	2.6	0.0
2.	Cu-1	46.1	24.4	26.4	2.6	0.5
3.	Cu-2	46.1	24.4	25.9	2.6	1.0
4.	Cu-3	46.1	24.4	25.4	2.6	1.5
5.	Cu-4	46.1	24.4	24.4	2.6	2.5

6.3 Results and discussion

6.3.1 Mechanical properties

6.3.1.1 Density and compressive strength

The results in Table 6.2 show the density, compressive strength and elastic moduli of bioactive glass samples. It was evident that the densities of the samples were found to increase from 2.72 to 2.86 gm/cc with increasing CuO content into the bioactive glass samples. The increase of CuO in the base bioactive glass (45S5) leads to an increase its density because of replacement of a lighter element, Ca (density = 1.55 g/cm^3) with a heavier element, Cu (density = 8.96 g/cm^3) (Tripathi *et al*., 2016).

Table 6.2: Density, compressive strength and elastic moduli of bioactive glass samples.

Sl No.	Sample's Code	Density (gm/cc)	Compressive Strength (MPa)	Young's Modulus (GPa)	Shear Modulus (GPa)	Bulk Modulus (GPa)
1.	45S5	2.72	53	76.74	30.43	53.77
2.	Cu-1	2.76	55	78.10	31.02	54.22
3.	Cu-2	2.79	56	79.95	31.91	55.93
4.	Cu-3	2.81	59	80.89	33.08	56.96
5.	Cu-4	2.86	64	82.21	35.25	59.09

Fig. 6.1 shows the compressive strength of bioactive glass samples in the form of error bars and from this Fig., it is also clear that with increasing amount of CuO the compressive strength of samples has increased from 53 to 64 MPa. This can be easily understood that greater the density of glass more would be the compactness of glass structure and consequently higher the compressive strength (Srivastava *et al*., 2012).

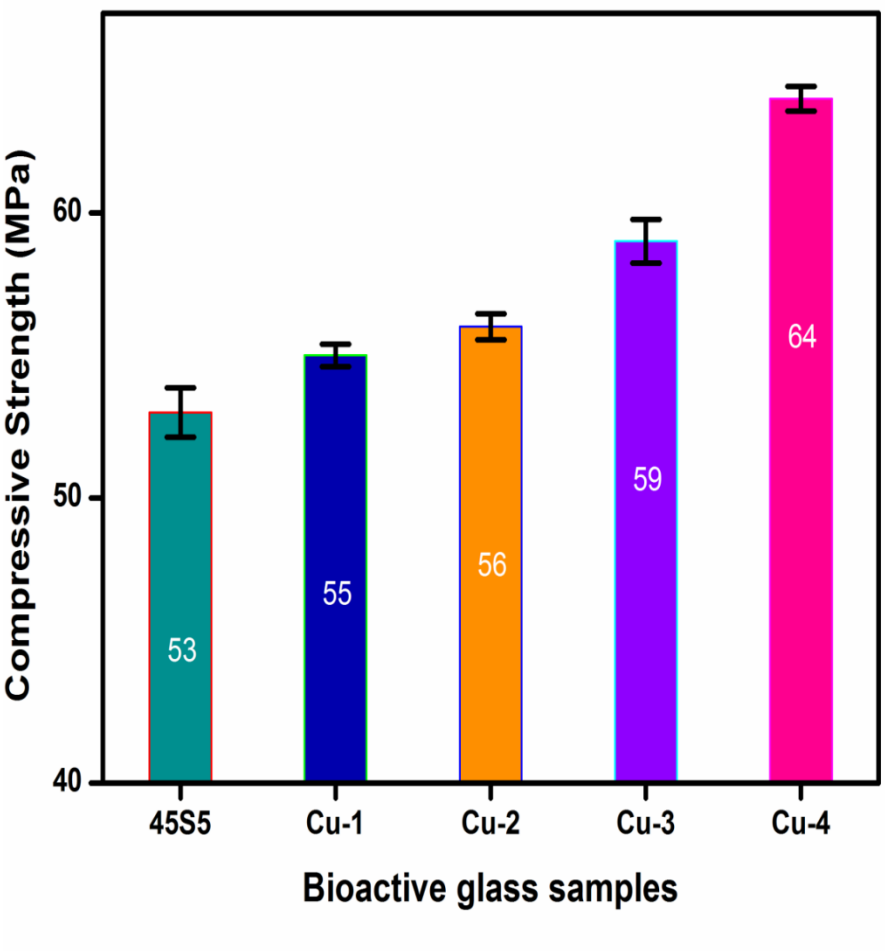

Fig. 6.1: Variation of compressive strength with composition of the bioactive glass samples (45S5 to Cu-4).

6.3.1.2. Elastic modulus, shear modulus and bulk modulus

Table 6.2 and Fig. 6.2 represent the experimental values of elastic moduli such as Young's modulus (E), shear modulus (S) and bulk modulus (K) of the bioactive glass samples. An increase in longitudinal and shear ultrasonic wave velocities as well as Young's, shear and bulk modulus of 45S5 bioactive glass is due to an increase of CuO content in it. Thus there is an increase in the elastic modulus of all glass samples with increasing CuO content as shown in Fig. 6.2.

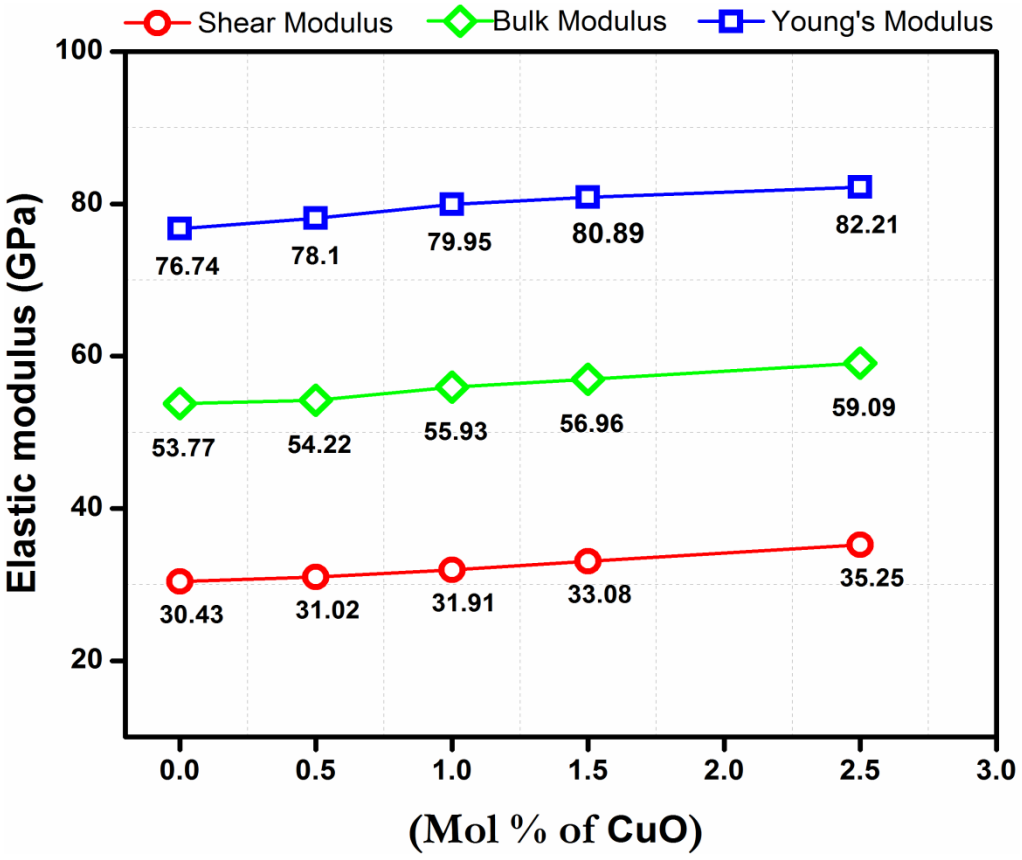

Fig. 6.2: Variation in elastic modulus, shear modulus and bulk modulus of all bioactive glass samples (45S5 to Cu-4) with CuO content.

It can be explained by decrease in the inter - atomic spacing which means that copper ions with octahedral coordination are involved in the glass network as modifiers by occupying the interstitial positions which cause an increase in the average number of the network bonds per unit volume. Therefore, it can be suggested that CuO modification leads to an increase in the network connectivity of the studied bioactive glasses (Paul, 1990). So, the incremental addition of CuO at the cost of CaO increases the modifier's concentration in the bioactive glass which increases the compactness of the glass structure also resulting in an increase in the Young's modulus (E), shear modulus (S) and bulk modulus (K) of the CuO doped bioactive glass samples.

So, finally it can be concluded that the doping of CuO for CaO in 45S5 glass system has increased its physical and mechanical properties.

6.3.2 *In vitro* bioactivity of bioactive glasses by X-ray difractometry

Fig. 6.3 represents the XRD patterns of the prepared bioactive glass samples (45S5, Cu-1, Cu-2, Cu-3 and Cu-4). The Fig 6.3 shows that before being soaking in SBF solution, there was no XRD peak for the bioactive glass samples, except a hump like peak ranging from 20° to 30° as it is attributed due to Si–O–Si network. So, it is clear that bioactive glass samples were amorphous in nature before being soaked in SBF solution (Brovarone *et al*., 2006). Fig. 6.4 shows the XRD patterns of the bioactive glass samples soaked in the SBF solution for 14 days.

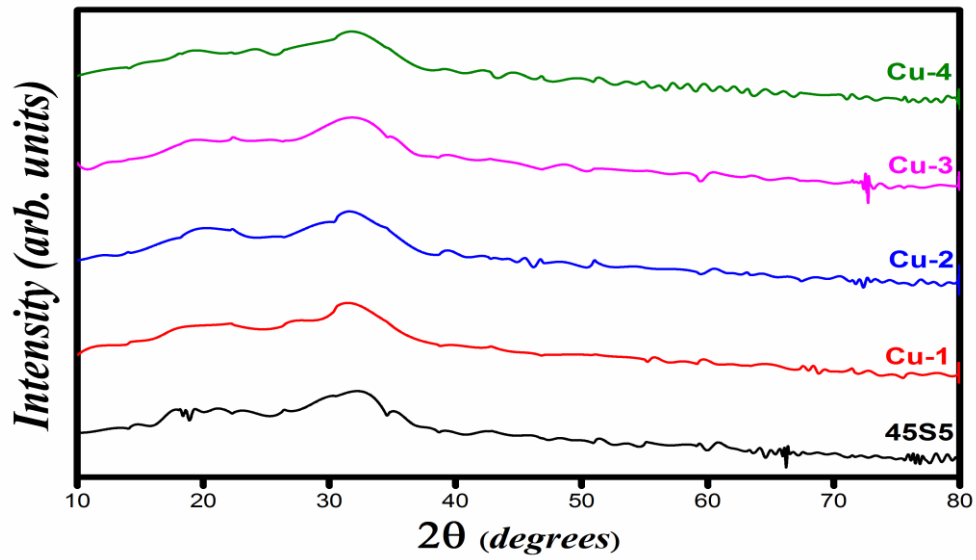

Fig. 6.3: XRD patterns of the bioactive glass samples (45S5 to Cu-4) before soaking them into the simulated body fluid (SBF) solution.

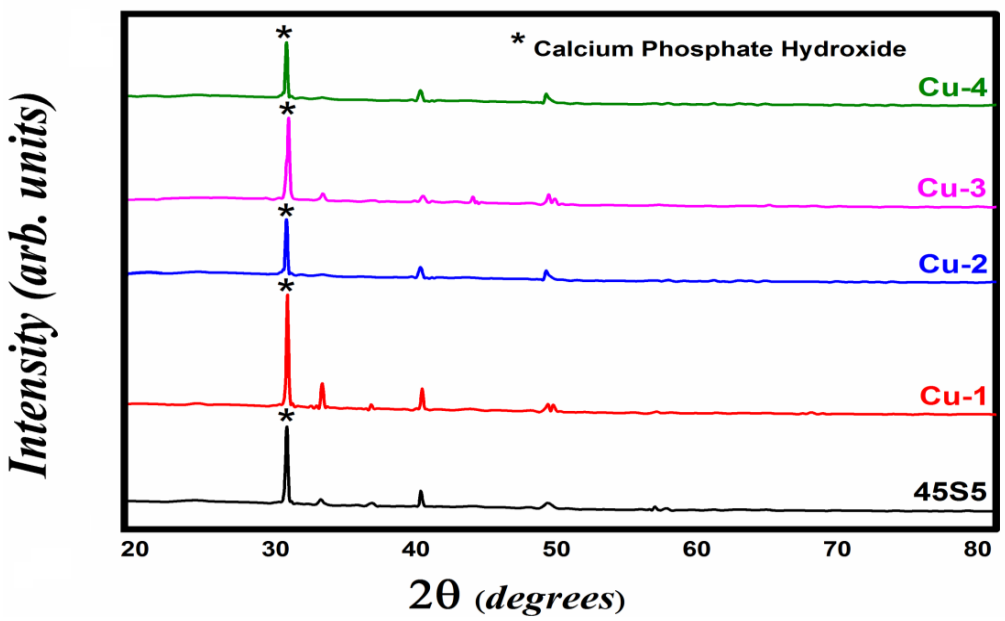

Fig. 6.4: XRD patterns of the bioactive glass samples (45S5 to Cu-4) soaked in the simulated body fluid (SBF) solution for 14 days.

After SBF treatment for 14 days, the diffraction patterns of all bioactive glass samples have shown sharp peaks at 31.7° which is due to the presence of calcium phosphate hydroxide matched with PDF no. 831886. These peaks were regarded as crystalline nature of HCA nucleated in presence of the solution (Fujiabayashi *et al*., 2003 and Kokubo *et al*., 2003). Therefore, this present system favours the HCA formation which has been also proved by the SEM and FTIR spectrometry.

6.3.4 SEM analysis of bioactive glass samples.

6.3.4.1 SEM analysis of bioactive glass samples before soaking in SBF solution

The SEM micrographs of 45S5 bioglass and CuO doped bioglass samples before soaking in SBF solution have been presented in Fig. 6.5 (a–e) which shows different rod type structures and irregular grains of bioactive glass samples similar to the results observed by Tripathi *et al*. (Tripathi *et al*., 2015).

Fig. 6.6 (a–e) shows the SEM micrographs of bioactive glass samples after soaking in SBF solution for 28 days. On SBF treatment HCA clusters change in a finer structure after 28 days of soaking due to partial dissolution and re-precipitation phenomena in solution. This happens due to solution refreshing and demonstrating the formation of a continuous layer of HCA (Tripathi *et al*., 2015 and Sampath *et al*., 2015).

A change in surface morphology is seen if it is compared with the initial surface of the bioactive glass samples. The SEM micrographs demonstrate that spherical particles have covered the surface of the bioactive glasses with variable shape and size. Therefore, the SEM pictures further confirm the growth of HCA layer on the surface of the samples after immersing in SBF solution.

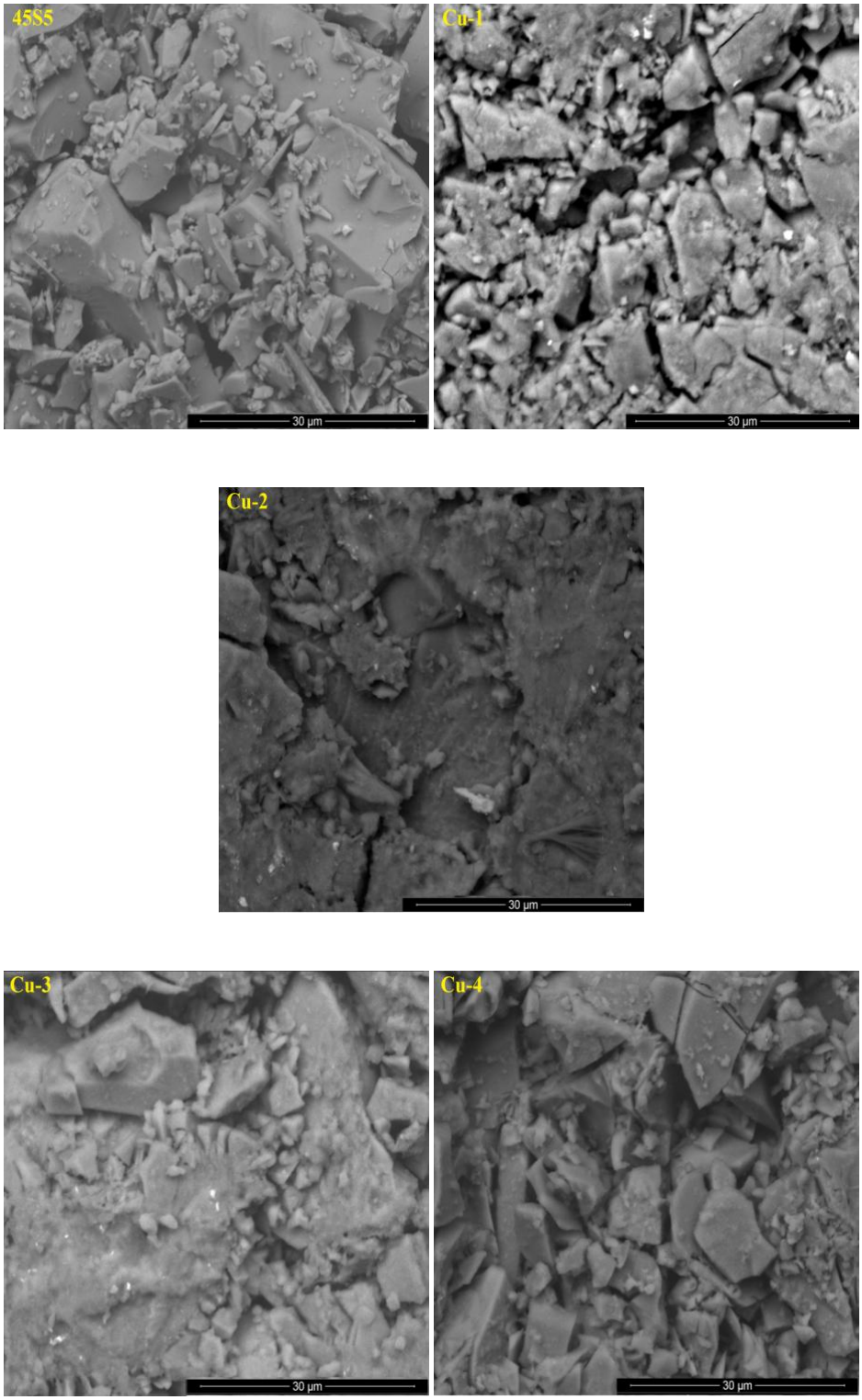

Fig. 6.5(a-e): SEM micrographs of bioactive glass samples (45S5 to Cu-4) before soaking in SBF solution.

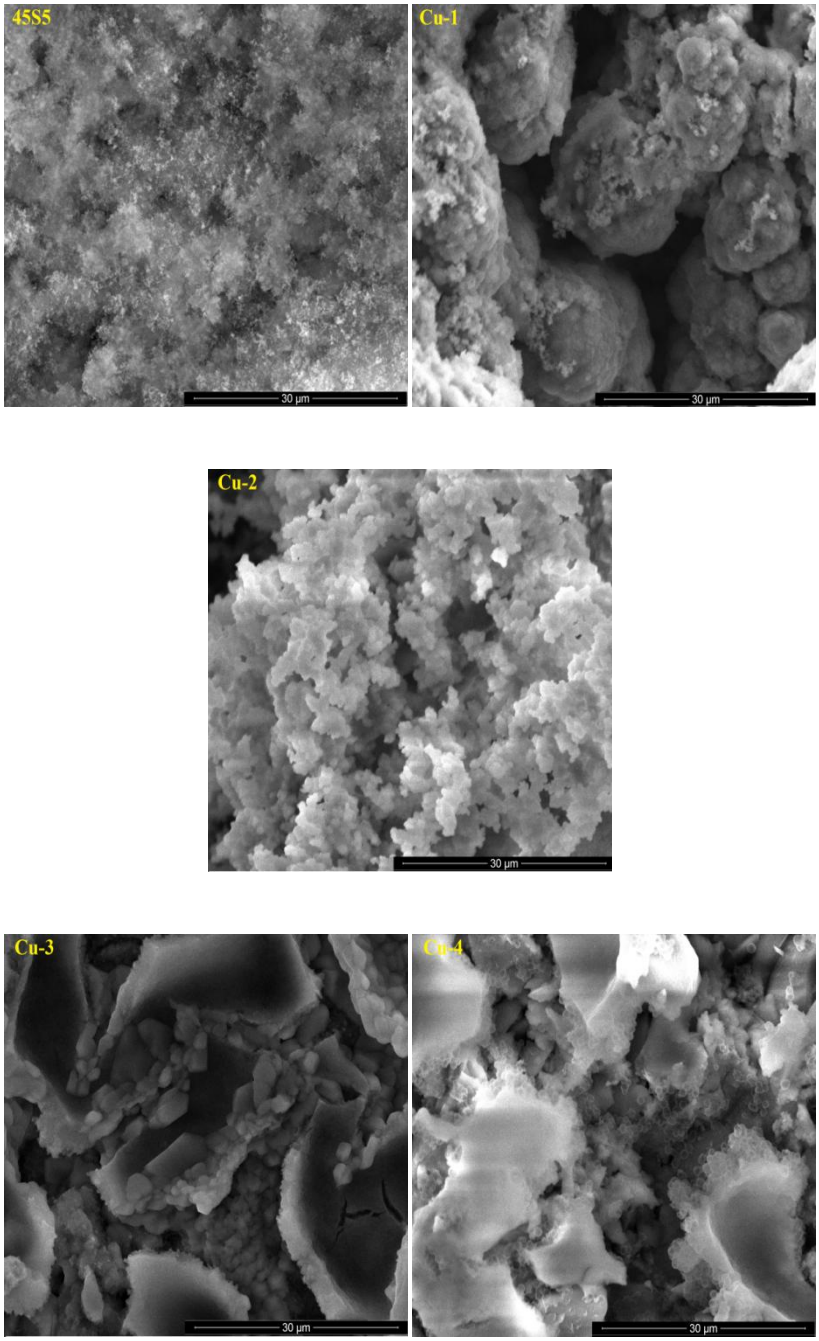

Fig. 6.6(a-e): SEM micrographs of bioactive glass samples (45S5 to Cu-4) after soaking in SBF solution.

On SBF treatment, HCA clusters change in a finer structure after 28 days of soaking due to partial dissolution and re-precipitation phenomena in solution. As pointed out earlier

this happened due to solution refreshing and demonstrating the formation of a continuous layer of HCA (Verne *et al*., 2005). So, after comparing these micrographs it can be concluded that the micrographs have shown the formation of HCA on the surface of bioactive glass samples after immersion in SBF solution for 28days. It was also observed that the numbers of HCA crystals were more on the surfaces of Cu-1, Cu-2 and Cu-3 as compared to other bioactive glasses. This significant development of HCA crystals might be associated with a high deposition of Ca-P layer and this is in good agreement with the XRD data (Fig. 6.4). Higher amount of CuO in Cu-4 decreases the formation of HCA as compared to other glass samples. So, for better bioactivity of these glass samples the amount of copper should be limited up to 1.5 mol% addition of CuO.

6.3.5 *In vitro* analysis of bioactive glass samples in SBF solution

Fig. 6.7 shows the variation of pH of bioactive glass samples after immersing in SBF solution for 1 to 28 days. It shows that for all bioactive glass samples, the pH increases within 1 to 3 days as compared to the initial pH of the SBF solution at 7.4 under physiological condition. The increase in pH values is due to fast release of cations through exchange with H^+ or H_3O^+ ions in the simulated body fluid (SBF) solution. The H^+ ions are being replaced by cations which cause an increase in hydroxyl concentration of the solution. This leads to attack on the silica glass network, which results silanols formation leading to decrease in pH after 3 days as indicated in the Fig. 6.7 when bioactive glass samples were immersed in simulated body fluid (SBF) solution up to 28 days. The maxima of pH values were recorded on the third days as pH 9.75, 10.06, 10.51, 9.59 and 9.29 for all the samples 45S5-Cu-4, respectively at 37°C under physiological condition, which is due to the fast dissolution rate. High degradation rate leads to higher

pH value. So, an increase in the pH value of SBF solution also favors the hydroxy carbonate apatite formation.

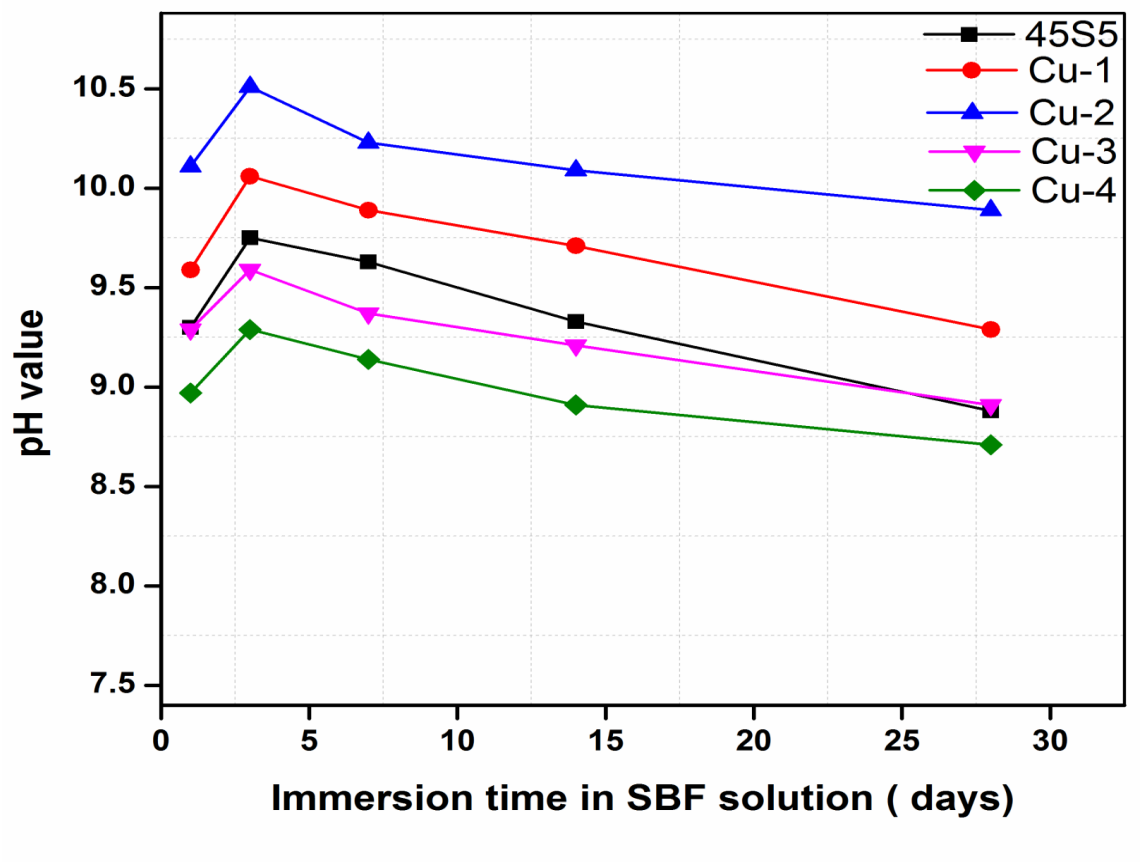

Fig. 6.7: Variation of pH of bioactive glass samples (45S5 to Cu-4) after immersing in SBF up to 28 days.

The dissolution rate as well as pH increment decreased after 4 days due to decrease of Na^{+} and Ca^{2+} ionic concentrations from sample surface. The reason for this decrease in the pH can be considered due to precipitation of Ca^{2+} ions from the solution to form calcium phosphates and carbonates. Moreover, the sample numbers Cu-1 and Cu-2 with lower CuO content were found to posses the highest rate of dissolution and hence the maximum pH values were recorded as compared with 45S5 bioglass. The incorporation

of CuO into 45S5 bioactive glass resulted in an increase in the pH of SBF. Their high degradation rate has led to a higher pH value and favored an early development of hydroxy carbonate apatite layer on the sample surface. As it is known that high concentration of Cu in glass increases its chemical durability and decreases dissolution property of glass samples and thus the samples, Cu-3 and Cu-4 have a lower pH in comparison to 45S5, Cu-1 and Cu-2 samples (Julian *et al*., 2015). Therefore, the results demarcate that the substitution of CuO for CaO in the present investigation did not alter the bioactivity mechanism in SBF.

6.3.6 FTIR-spectrometry

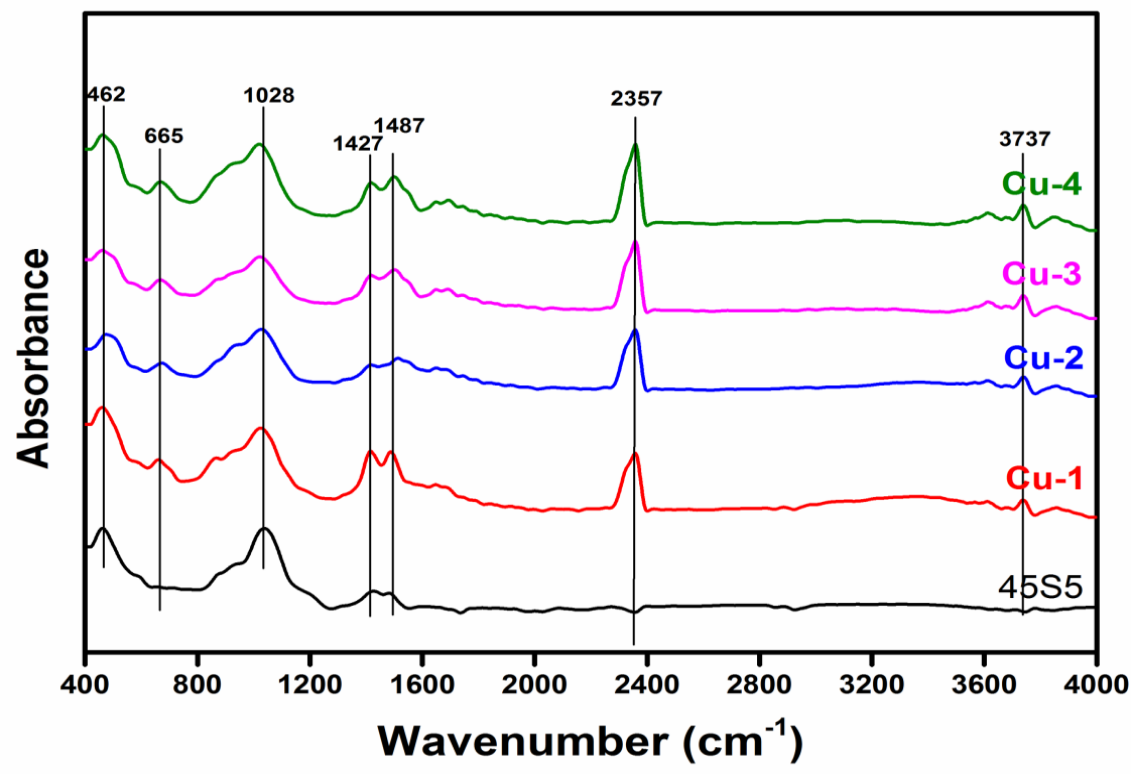

Fig. 6.8: FTIR absorption spectra of all glass samples (45S5 to Cu-4) before soaking them into SBF solution.

Fig. 6.8 shows the Fourier transform infrared (FTIR) absorption spectra of the bioactive glass samples recorded in the wavenumber range of 400–4000 cm^{-1} on the FTIR spectrometer before SBF treatment. The 45S5 base bioglass has revealed the FTIR absorption bands at 462, 665, 1028, 1427, 1487, 2357 and 3737 cm^{-1}. The spectral bands of Cu-1, Cu-2, Cu-3 and Cu-4 samples have shown a similar behavior like 45S5, with small variations in the band intensities. The resultant FTIR band centered at around 462 cm^{-1} is associated with a Si–O–Si symmetric bending mode of vibration. The absorption peak at about 665 cm^{-1} is assigned due to Si-O stretching mode of vibration. The absorption peak observed at 1028 cm^{-1} can be attributed to Si-O-Si asymmetric stretching mode of vibration in the silicate tetrahedral network.

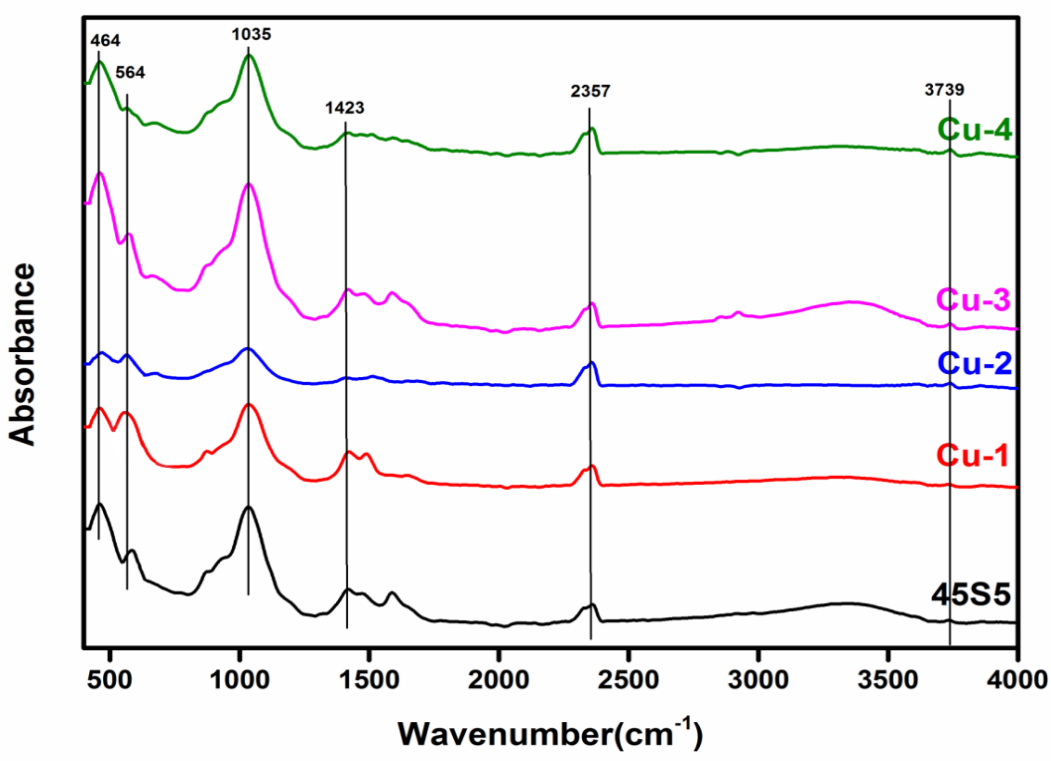

Fig. 6.9: FTIR absorption spectra of all glass samples (45S5 to Cu-4) after soaking them into SBF for 7 days.

The bands at 1427 cm^{-1} and 1487 cm^{-1} correspond to C-O stretching mode which might have appeared due to reaction between the glass and carbon dioxide present in the atmosphere. Fig. 6.9 shows the Fourier transform infrared (FTIR) absorption spectra of the bioactive glass samples recorded in the wavenumber range of 400–4000 cm^{-1} on the FTIR spectrometer after 7 days of SBF treatment. After immersion of samples in SBF for 7 days, the new bands appeared at 564 cm^{-1}, as shown in Fig. 6.9. The bands centered at 564 cm^{-1} are attributed to the P-O bending mode of vibrations. These characteristic bands represent the formation of hydroxyl carbonate apatite (HCA) layer on the surface of the bioactive glass samples. It is quite evident from the spectra that the intensities of the phosphate groups (564 cm^{-1}) have increased in these bioactive glasses as shown earlier by previous workers (Chickerur *et al*. 1980). Therefore, the results suggest that the HCA layer formation has taken place on the surface of glass samples. The prolonged period of treatment of the sample in SBF has also shown the similar behavior favorably due to formation of hydroxyl carbonate apatite (HCA) layer.

6.3.7 Antibacterial tests

Antibacterial property of bioglass samples (45S5, Cu-1, Cu-2 and Cu-3) were investigated using quantitative viable count method. All samples at concentration 10 mg/mL were incubated with E. coli suspension for 24h (Fig. 6.10). This antibacterial effect of glass samples are attributed to the increase in pH level which has reduced the viability of bacterial suspension. However, in this study 45S5 bioglass showed no antibacterial effect whereas sample, Cu-1 with minimum concentration of CuO showed very small effect towards E. coli which was attributed to a very low concentration (10 mg/mL) of samples used for this test. Whereas at the same time Cu-2 and Cu-3 samples

had shown significant antibacterial effect due to the presence of increased concentration of Cu^{2+} ion. Copper ions have been reported to bind rapidly to E. coli cells, inhibit endogenous respiration of cells as well as penetrate into the cytoplasm of the cells and interfere with their metabolic functions.

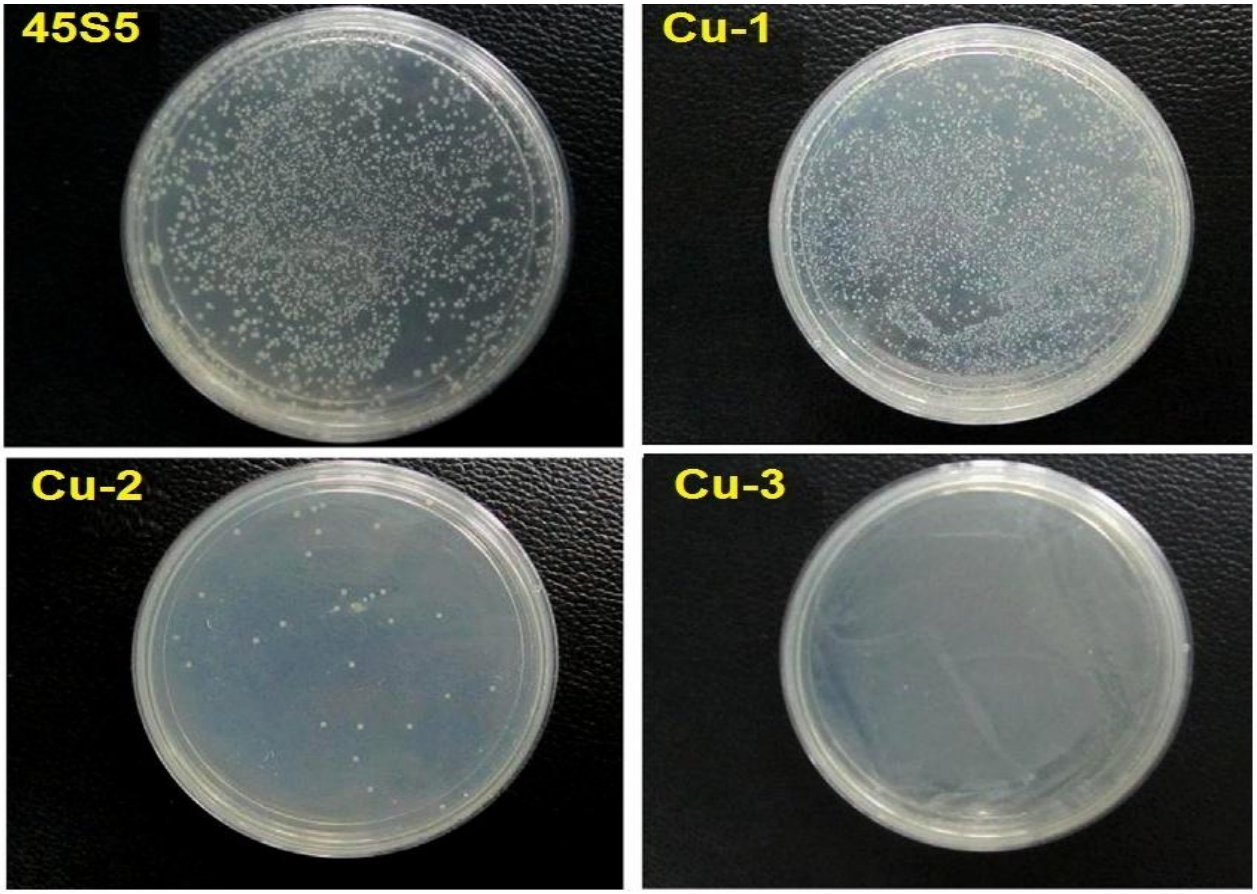

Fig. 6.10: Antibacterial effect of bioglass samples 45S5, Cu-1, Cu-2 and Cu-3 towards E. coli suspension for 24 hrs.

It is expected that the interference of metabolic activity in the cell is due to the rapid combination of Cu^{2+} ions with phosphate and protein compounds. Attachment of copper particle at the surface of cells could block the transport of essential nutrients leading to cell death and might induce mechanical damage to the cell membrane. In short, the direct

contact of copper particles and bacterial cells is the crucial factor to explain the toxicity of copper towards E. coli. The CuO doped 45S5 bioglasses synthesized in this study are considered to possess better antibacterial properties than 45S5 glass because it can act through two distinct mechanisms such as ionic and particle effects. This is particularly important because in case one of the mechanisms was impeded due to environmental factor, e.g. particle effects diminished upon interaction or agglomeration with other particles in the medium (Thin *et al*., 2006), ionic effect could help to retain the antibacterial function of the material. So, it can be mentioned that copper doped 45S5 bioglasses show antibacterial effect which can be used to prevent bacterial infection in dental and orthopedic bone implants.

6.4 Conclusions

In the present investigation, a comparative study was made on physical, bioactive, mechanical and antibacterial properties of CuO substituted 45S5 bioactive glasses. The following conclusions are obtained from this investigation:

1. On increasing the substitution of CuO for CaO in the bioactive glass 45S5, density, compressive strength and elastic modulus were found to increase accordingly.
2. The FTIR absorption spectra showed different characteristics band because of silicate network which indicated the formation of the hydroxy calcium apatite (HA) layer on the surface of bioactive glass samples after immersing in SBF from 1 to 7 days.

3. The bioactivity of these samples was measured by in-vitro analysis in SBF solution for 1 to 28 days. The pH of the solution was found to increase from 1 to 3 days and nearly constant up to 7 days. After 7 days the pH of the glass samples decreased that shows the samples were bioactive. An increase in the pH of the SBF shows the relative increase in bioactivity of the sample immersed in the solution.
4. The SEM analysis of these samples before soaking in SBF shows the different irregular grains of glass samples. While after 28 days of SBF treatment, HA layer was formed on the surface of these samples due to its bioactive nature.
5. Incorporation of Cu of above 0.5 mol% was able to impart bioglass with antibacterial properties. Antibacterial test using quantitative viable count method showed that Cu-2 and Cu-3 samples prevent bacterial colonization effectively after 24 h.

Thus, we can say that substitution of CuO for CaO in the bioactive glass 45S5 would be good bioactive and antibacterial materials which have better mechanical properties with the comparison to bioactive glass 45S5.

References:

Aina V, Malavasi G, Pla AF, Munaron L and Morterra C, Zinc - containing bioactive glasses: Surface reactivity and behaviour towards endothelial cells, Acta Biomaterialia, 5, 1211 –1222, 2009.

Arredondo M and Núñez MT, Iron and copper metabolism, Mol Aspects Med, 26, 313–327, 2005.

Best SM, Porter AE, Thian ES and Huang J, Bioceramics: Past, present and for the future, Journal ofthe European Ceramic Society, 28, 1319 –1327, 2008.

Brovarone C Vitale, Verne E and Appendino P, Macroporous bioactive glass-ceramic scaffolds for tissue engineering, J Mater Sci Mater Med, 17, 1069–1078, 2006.

Chen QZ, Thompson ID and Boccaccini AR, 45S5 Bioglasss-derived glass–ceramic scaffolds for bone tissue engineering, Biomaterials, 27, 2414–2425,2006.

Chickerur NS, Tung MS and Brown WE, A mechanism for incorporation of carbonate into apatite, Calcified Tissue International, 32, 55–62, 1980.

Erol M, Özyu A, Mara M and Küçükbayrak S, *In vitro* evaluation of Sr and Cu doped bioactive glasses, Adv Sci Lett19, 3333–3337, 2013.

Espirito Santo C, Taudte N, Nies DH and Grass G, Contribution of copper ion resistance to survival of Escherichia coli on metallic copper surfaces, Appl Environ Microbiol 74, 977–986, 2008.

Finney L, Vogt S, Fukai T and Glesne D, Copper and angiogenesis: unravelling a relationship key to cancer progression, Clin Exp Pharmacol Physiol, 36, 88–94, 2009.

Fujiabayashi S, Neo M, Kim HM, Kokubo T and Nakamura T, A comparative study between *in vivo* bone in growth and *in vitro* apatite formation on $Na_2O–CaO–SiO_2$ glasses, Biomaterials, 24, 1349–1356, 2003.

Gérard C, Bordeleau LJ, Barralet J and Doillon CJ, The stimulation of angiogenesis and collagen deposition by copper, Biomaterials, 31, 824–831, 2010.

Gosheger G, Hardes J, Ahrens H, Streitburger A, Buerger H, Erren M, Gunsel A, Kemper FH, Winkelmann W, Von Eiff C, Silver-coated megaendoprostheses in a rabbit model--an analysis of the infection rate and toxicological side effects, Biomaterials, 25, 5547–5556, 2004.

Grass G, Rensing C and Solioz M, Antimicrobial metallic copper surfaces kill *Staphylococcus haemolyticus* via membrane damage, Appl Environ Microbiol, 77, 1541–1547, 2011.

Hench LL and Andersson O, An Introduction to Bioceramics, World Scientific press, Singapore, 41, 1993.

Hoppe A, Güldal NS and Boccaccini AR, A review of the biological response to ionic dissolution products from bioactive glasses and glass–ceramics, Biomaterials, 32, 2757–2774, 2011.

Jarcho M, Kay JL, Gumaer RH and Drobeck HP, Tissue, cellular and sub cellular events at bone – ceramic hydroxyapatite interface, Journal of Bioengineering, 1, 79 – 92, 1977.

Julian Bejarano, Pablo Caviedes and Humberto Palza, Sol–gel synthesis and *in vitro* bioactivity of copper and zinc-doped silicate bioactive glasses and glass-ceramics, Biomed Mater, 10, 025001, 2015.

Kokubo T, Ito S, Huang ZT, Hayashi T, Sakka S, Kitsugi T and Yamamuro T, Ca, P - rich layer formed on high strength bioactive glass-ceramic A - W., Journal of Biomedical Materials Research, 24, 331 - 343, 1990.

Kokubo T, Kim HM and Kawashita M, Novel bioactive materials with different mechanical properties, Biomaterials, 24, 2161–2175, 2003.

Kokubo T and Takadama H, How useful is SBF in predicting in vivo bone bioactivity?, Biomaterials, 27, 2907–2915, 2006.

Lakhkar NJ, Lee IH, Kim HW, Salih V, Wall IB and Knowles JC, Bone formation controlled by biologically relevant inorganic ions: role and controlled delivery from phosphate-based glasses, Adv Drug Deliv Rev, 65, 405–420, 2012.

Lee HJ and Jeong SH, Acteriostasis and skin innoxiousness of nano size silver colloids on textile fabrics, Textile Research Journal, 75, 551–556, 2005.

Lin CC, Huang LC and Shen P, $Na_2CaSi_2O_6$ - P_2O_5 based bioactive glasses. Part 1: Elasticity and structure, Journal of Non - Crystalline Solids, 351, 3195 -3203, 2005.

Mazrooei Sebdani M, Fathi MH, Novel hydroxyapatite-forsterite bioglass nano composite coatings with improved mechanical properties, Journal of Alloys and Compounds, 509, 2273–2276, 2011.

Morrier JJ, Suchett-Kaye G, Nguyen D, Rocca JP, Blanc-Benon J and Barsotti O, Antimicrobial activity of amalgams, alloys and their elements and phases, Dent Mater, 14, 150–157, 1998.

Noyce JO, Michels H, and Keevil CW, Potential use of copper surfaces to reduce survival of epidemic methicillin-resistant *Staphylococcusaureus* in the healthcare environment, J Hosp Infect, 63, 289–297, 2006.

Ogino M and Hench LL, Formation of calcium phosphate films on silicate glasses, Journal of Non -Crystalline Solids, 38, 673 – 678, 1980.

Ohtsuki C, Kokubo T and Yamamuro T, Mechanism of apatite formationon $CaO–SiO_2–P_2O_5$ glasses in a simulated body fluid, Journal of Non-Crystalline Solids, 143, 84–92, 1992.

Paul A, Chemistry of Glasses (London: Chapman & Hall) 2nd ed., 149–151, 1990.

Palza H, Escobar B, Bejarano J, Bravo D, Diaz-Dosque M and Perez J, Designing antimicrobial bioactive glass materials with embedded metal ions synthesized by the sol–gel method, Mater Sci Eng C, 33, 3795–3801, 2013.

Pye AD, Lockhart DEA, Dawson MP, Murray CA and Smith AJ, A review of dental implants and infection, Journal of Hospital Infection,72, 104–110, 2009.

Rejda BV, Peelen JGJ and Groot K de, Tricalciumphosphate as a bone substitute, Journal of Bioengineering, 1, 93-97, 1977.

Rupp ME, Fitzgerald T, Marion N, Helget V, Puumala S, Anderson JR and Fey PD, Effect of silver-coated urinary catheters: efficacy, cost-effectiveness, and antimicrobial resistance, J Infect Control, 32, 445–450, 2004.

Sampath Kumar Arepalli, Tripathi Himanshu, Vyas Vikash Kumar, Kumar S Shyam, Jain Shubham, Pyare Ram and Singh SP, Influence of barium substitution on bioactivity, thermal and physico-mechanical properties of bioactive glass, Material Science and Engineering C, 49, 549-559, 2015.

Schrand AM, Rahman MF, Hussain SM, Schlager JJ, Smith DA and Syed AF, Metal-based nano particles and their toxicity assessment, Nanomed Nano biotechnol, 2, 544–568, 2010.

Srinivasan S, Jayasree R, Chennazhi KP, Nair SV, Jaya kumar R, Biocompatible alginate/nano bioactive glass ceramic composite scaffolds forperiodontal tissue regeneration, Carbohydrate Polymers, 87, 274–283, 2012.

Srivastava A K and Pyare R, Characterization of CuO substituted 45S5 bioactive glasses and glass—ceramics, Int J Sci Technol Res, 1, 28–41, 2012.

Thill A, Zeyons O, Spalla O, Chauvat F, Rose J, Auffan M and Flank AM, Cytotoxicity of CeO_2 nanoparticles for Escherichia coli. Physico-chemical insight of the cytotoxicity mechanism, Environmental Science and Technology, 40, 6151–6156, 2006.

Tripathi Himanshu, Hira Sumit Kumar, Kumar Arepalli Sampath, Gupta Uttam, Manna Partha Pratim and Singh SP, Structural characterization and in vitro bioactivity assessment of SiO_2–CaO–P_2O_5–K_2O–Al_2O_3 glass as bioactive ceramic material, Ceramics International, 41, 11756–11769, 2015.

Tripathi Himanshu, Kumar Arepalli Sampath and Singh SP, Preparation and characterization of Li_2O–CaO–Al_2O_3–P_2O_5–SiO_2 glasses as bioactive material, Bulletin of Material Science, 39(2), 365–376, 2016.

Varmette EA, Nowalk JR, Flick LM and Hall MM, Abrogation of the inflammatory response in LPS-stimulated RAW 264.7 murine macrophages by Zn and Cu-doped bioactive sol–gel glasses, J Biomed Mater Res, Part A, 90, 317–325, 2009.

Verne E, Nunzio S Di, Bosetti M, Appendino P, Brovarone C Vitale, Maina G and Cannas M, Surface characterization of silver-doped bioactive glass, Biomaterials, 26, 5111–5119, 2005.